Journal of Polymer Research (2022) 29: 172
https://doi.org/10.1007/s10965-022-03007-4

ORIGINAL PAPER

Beta-FeOOH/polyamide nanocomposites for the remediation of 4-chlorophenol from contaminated waters

Michael Ovbare Akharame[1,2] · Ogheneochuko Utieyin Oputu[1] · Omoniyi Pereao[3] · Daniel Ikudayisi Olorunfemi[2] · Olalekan Siyanbola Fatoki[1] · Beatrice Olutoyin Opeolu[3]

Received: 28 October 2021 / Accepted: 29 March 2022 / Published online: 19 April 2022

Abstract

The safe application of nanoparticles in water treatment processes is a growing concern globally, making the utilisation and deployment of appropriate support materials necessary. Hydrothermally synthesised β-FeOOH nanoparticles were incorporated into the polyamide matrix via an in-situ method to fabricate catalytic composites. The materials elucidation was effected using SEM, TEM, ATR-FTIR, XRD and nitrogen adsorption–desorption. The heterogeneous catalytic property of the β-FeOOH/polyamide nanocomposites was evaluated in an aqueous ozonation system with 4-chlorophenol (4CP) as the target organic pollutant. Aliquots were drawn at different time intervals and analysed by LCMS-TOF. The results showed high degradation of 4CP (98.52%) within 40 min compared with ozonation (62.94%). The degradation of 4CP under pH 3, 7 and 10 gave efficiencies of 83.56%, 90.16% and 96.01%, respectively, at 30 min. The composite exhibited excellent reuse potential over six cycles, with no iron leaching observed at different pH conditions. The chemical oxygen demand (COD) and total organic carbon (TOC) for natural wastewater were reduced by 54.62% and 89.22% respectively using the polymeric nanocomposites, while the optimum treatment duration was established using ecotoxicity assessment of the treated water. The novel composites gave excellent removal of 4CP from aqueous solutions.

Keywords Beta-FeOOH · Polyamide · 4-chlorophenol · Wastewater remediation · Regeneration · Toxicity assessment

Introduction

Phenol and its various derivatives have been reported to be active endocrine-disrupting chemicals [1, 2]. Their toxicity is related to perceived hydrophobicity, the ready formation of free radicals, and easy localisation of substituents [3], with adverse effects on both plants and animals [4, 5]. The ubiquitous 4-chlorophenol (4CP) is currently regarded as a priority pollutant due to its toxic nature and biodegradation resistance, making it difficult to remove from the environment, especially aqueous systems [6]. It has been reported to possess carcinogenic and mutagenic properties [7–11]. The xenobiotic tendencies of the compound and its persistence in environmental matrices make it a significant pollutant of interest to researchers in the global scientific community.

Water contamination with organic compounds such as endocrine-disrupting chemicals (EDCs) and persistent organic pollutants (POPs) poses challenges to conventional wastewater treatment processes [12], especially when the goal is possible reuse of the treated water. In the last decade, rapid and significant progress has been made in the design of advanced technologies and procedures for wastewater treatment to eliminate pollution and increase pollutants destruction or separation processes [13, 14]. In particular, nanoparticles, nanomaterials, and their composites to remediate and disinfect wastewater have gained much interest [15–22]. Iron and its oxides (i.e. oxides, hydroxides and oxyhydroxides) are among the plethora of nanomaterials employed in nano-based water treatment operations. Oxides of iron possess high energy of crystallisation and therefore form minute crystals. The high crystallinity accounts for the high specific surface area, making them effective sorbents and reactive oxidants [23].

✉ Michael Ovbare Akharame
michael.akharame@uniben.edu

[1] Department of Chemistry, Cape Peninsula University of Technology, Cape Town 8000, South Africa

[2] Department of Environmental Management and Toxicology, University of Benin, Benin-City 3002, Nigeria

[3] Department of Environmental and Occupational Health, Cape Peninsula University of Technology, Cape Town 8000, South Africa

Beta iron oxyhydroxide nanoparticles (β-FeOOH), also known as akaganéite, are among the numerous oxides of iron. It is a non-toxic, relatively cheap, and easy to synthesise anti-ferromagnetic material with high surface area and narrow pore size distribution [24]. The catalytic property of β-FeOOH has been established in the degradation of organic pollutants [25, 26]. It has also been used to form composites with other materials for enhanced catalytic performance and operational resilience; these support materials include $BiVO_4$ [27], NiO [28], TiO_2 [29, 30], reduced graphene oxide [31], graphitic carbon nitride [32], etc. Some of these investigations reported operational challenges during the application processes, such as the dissolution of Fe, difficult recovery of the nanoparticles after use, and the limited regeneration and reuse cycles [26, 28].

Polymeric nanocomposites (PNCs) are widely embraced hybrid materials utilised to remediate and monitor wastewater [33, 34]. Their enhanced properties include improved membrane permeability, fouling resistance, mechanical and thermal stability, higher adsorption, as well as photocatalytic activities [35]. Additionally, incorporating the nanomaterials into polymer matrices brings about some operational advantages compared to the use of bare nanoparticles or other inorganic support materials. The gains include the reduction/prevention of nanoparticles loss, ease of recovery and regeneration for reuse, and the subsequent safeguarding of our environment and the biota therein [36].

Herein, we report the development of novel PNC based on hydrothermally synthesised β-FeOOH in-situ supported on polyamide for the heterogeneous catalytic ozonation of the organic pollutant 4CP in aqueous media. The synthesised PNC eliminated Fe leaching with stability extending to six cycles. Furthermore, toxicity output was within acceptable limits. This novel PNC exhibited promising remediation capability for the target pollutant (4CP) and organics in natural wastewater. Polyamide was selected as support in this study because it possesses exceptional mechanical, abrasion, wear, barrier, and crystalline properties [37–40]. Its excellent hydrophilicity, as well as its thermal and chemical stability has enabled it to be used to fabricate water treatment membranes, adsorbents and catalysts [41–45]. Polyamides exhibit good compatibility with numerous nanomaterials [46], possessing reactive sites in their chains via the active amines and carboxylic acid groups [47] which serve as anchor points for incorporated nanomaterials. The polymer's major advantages are its cost-effectiveness, lightweight and enhanced load-resistant properties [48], and several established high-yield and relatively easy syntheses procedures [39].

From the literature search, to date only the polymer polyaniline has been utilised to support the β-FeOOH nanoparticles in water treatment operations [24, 49]. The composites were employed to remove Cd(II) and Cr(VI) via adsorption processes. To the best of our knowledge, this is the first attempt to apply the β-FeOOH/polyamide composite in a heterogeneous catalytic system to degrade organics. This paper aims to present β-FeOOH in a polymer matrix as a viable composite material to suppress its leaching/dissolution during use in catalytic ozonation.

Experimental

Chemicals

The analytical grade chemicals were used as received. The 4-chlorophenol (99%), ε-caprolactam (99%), 6-aminocaproic acid (99%), $FeCl_3.6H_2O$, NH_4OH (NH_3 content 28–30%), HCl (99.9%), ethanol (99.5%), formic acid (98%) and HPLC grade acetonitrile (> 98%) were purchased from Sigma Aldrich, South Africa. *Air-Liquide*, South Africa, supplied the oxygen (99.998%). Daphtoxkit FM™ *Magna* toxicity assay kits were obtained from Microbiotest Inc., Belgium. Milli-Q water-18 Ω (Milli-Q Academic, France) was used for all the experiments.

Synthesis of β-FeOOH nanoparticles

The β-FeOOH nanoparticles were synthesised using the method described by Chowdhury et al. [50]. Briefly, a 400 mL water/ethanol mixture (3:7) was first adjusted to pH 10 by dropwise addition of NH_4OH, followed by adding 1.62 g of $FeCl_3.6H_2O$ under stirring. The final pH of the mixture was then adjusted to be 2.0 using HCl (1 M). The homogenous mixture was placed in a 2 L Teflon lined pressure vessel, heated at 100 °C for 2 h and allowed to cool down to room temperature. The supernatant was decanted, and the residue (crystals) centrifuged, then copiously washed with ethanol to remove residual chloride ions and subsequently oven-dried at 60 °C overnight. Finally, the prepared β-FeOOH nanoparticles were stored in a desiccator.

Synthesis of β-FeOOH/polymer composites

The method for the preparation of the β-FeOOH/polyamide composites was modified from that described by O'Neill et al. [38]. Briefly, ε-caprolactam (30 g) was placed into a 50 mL round bottom flask with a magnetic stirrer and kept in a fume hood under an inert nitrogen atmosphere. The temperature was raised to 80 °C (internal temperature of the round bottom flask), with a magnetic flea added and set to a stirring speed of 1500 rpm during the polymerisation. The requisite amounts of synthesised β-FeOOH particles were added to give weight percentage (wt%) composites of 0.5 wt%, 0.75 wt%, 1.0 wt% and 1.25 wt%, respectively. After that, the temperature was increased to 150 °C. A 10 wt% (3 g) of the initiator (6-aminocaproic acid) was added,

and the reaction was allowed to continue for 30 min. Further temperature increases to 200 °C for 30 min, 225 °C for 30 min and 250 °C for 5 h were carried out.

The resulting viscous polymer was poured into boiling Milli-Q water and allowed to cool. The nanocomposite was then chopped into small pieces using a stainless-steel knife and washed with boiling water for 2 h. The washing was repeated four times to remove unreacted monomers. The thoroughly clean samples were then vacuum-dried overnight at 80 °C. Figure 1 gives the graphical representation for the synthesis of the β-FeOOH/polyamide composites.

Characterisation of β-FeOOH nanoparticles and polymeric nanocomposites

The infrared spectra of the synthesised materials were captured within the range of 4000–400 cm^{-1} using a UATR Two PerkinElmer FT-IR spectrometer (Llantrisant, UK). Nitrogen adsorption–desorption analysis for surface area, pore volume and pore size was carried out for the nanoparticles only with TriStar II 3020, Version 2.00 Unit. Powder XRD spectra were obtained using a Bruker D8 Advance powder diffractometer with Vantec detector and fixed divergence and receiving slits with Co-Kα radiation. The phases were identified using Bruker Topas 4.1 software [51], and the relative phase amounts (weight %) were estimated using the Rietveld method. SEM images were captured with a Nova NanoSEM 230 with a field emission gun and operated at an energy level of 5.0 keV. EDS spectrum was obtained with an Oxford X-Max 20mm^2 detector, and the data was collected using Oxford INCA software. TEM images were captured using an FEI Tecnai 20 transmission electron microscope (FEI, Eindhoven, Netherlands) operating at 200 kV (Lab6 emitter) and fitted with a Tridiem energy filter and Gatan CCD camera (Gatan, UK). Degassing of the samples was carried out at 35 °C for 24 h before the measurements.

Catalytic ozonation, regeneration and leaching studies

The concentration of 4CP was set at 2×10^{-3} M based on preliminary optimisation experiments that ensured the experimental duration was within a reasonable sampling protocol (60 min). Moreover, the chosen value accounted for the cumulative organic load of recalcitrant compounds, which would contribute to the chemical and biological oxygen demand. Theoretical COD for 2×10^{-3} M 4CP was calculated as 416 mg/O_2 L, which was close to moderately contaminated wastewater total COD load. Measuring the O_3 feed rate was done via sparging the generated O_3 into 2% KI solution [52] with 27.60 ± 0.91 mg/L obtained, which gave the O_3 feed rate of 8.28 ± 0.27 mg/h at 20 °C. [53, 54]. Preliminary adsorption of organic substrate on the β-FeOOH/polyamide was evaluated by dispersing 0.5 g of the nanocomposite into the analyte solution. The mixture allowed to attain equilibrium (t = 60 min) by stirring the reactor (without the infusion of O_3 gas) with samples drawn for analysis.

For the catalytic ozonation, 100 mL (2×10^{-3} M) of the analyte solution was introduced into a sintered glass reactor fitted with a porous glass spout (porosity of 2) for the sparging of 10 mL min^{-1} O_2/O_3 mixture from the O_3 generator (EcoTech, model 1000BT-12, South Africa). A catalyst loading of 0.5 g was used for each catalytic operation. Samples (1 mL) were collected over 60 min, and the residual substrate concentrations were analysed using an Ace 5 C18 column by LCMS-TOF (Agilent 6230 TOF LC–MS–Agilent Technologies, Inc, USA). The Agilent 1260 infinity series utilised comprised a binary pump, an auto-sampler and an 1100 diode array detector (DAD), operating on Mass Hunter software version 8.0. The mobile phases were 0.1% formic acid in water and 0.1% formic acid in acetonitrile (see SI Table S1 for the optimised gradient). The ionisation of the 4CP was carried out by electrospray (ESI) nebulised over a drying gas at 350 °C (nitrogen), with the negative mode utilised for the ions capturing, set to -175 V for the fragmentation voltage. The pH adjustment for the analyte solution was made using NaOH (0.5 M) and H_3PO_4 (0.5 M) for the alkaline and acidic adjustments, respectively. The experiments were performed under constant stirring (100 rpm) and at an operating temperature of 20 ± 1 °C.

The degradation efficiency was calculated using the equation:

$$Degradation\ efficiency\ (\%) = \frac{\left(C_{o-C_t}\right)}{C_O} \times 100\% \quad (1)$$

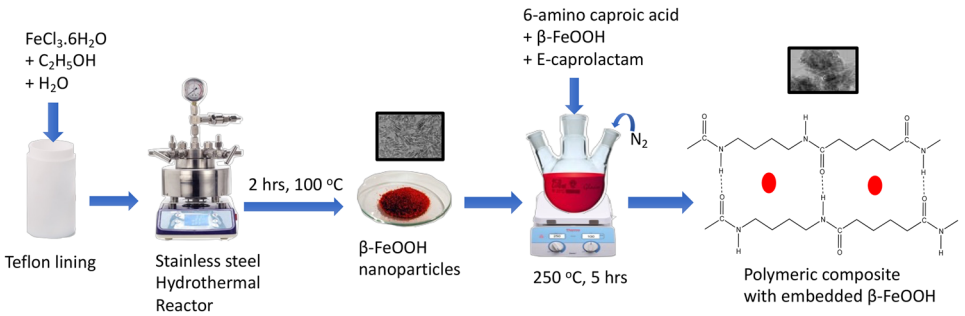

Fig. 1 Synthesis scheme of the β-FeOOH/polyamide nanocomposites showing suggested anchor points for the nanoparticles in the polymer matrix

where Co is the initial concentration of the analyte and Ct is the concentration removed at time t (min).

The data obtained from the catalytic ozonation of the 4CP at different pH (3, 7 and 10) were fitted into the pseudo-first-order kinetics model following the Langmuir-Hanshelwood model to determine the rate constant, respectively [55, 56].

$$ln = \left(\frac{c_o}{c_t}\right) = K_1 t \quad (2)$$

where *Co* is the initial concentration of analytes, *Ct* is the concentration removed at time *t* (min), and K_1 (min^{-1}) is the first-order rate constant.

The used nanocomposites were immersed in 50 mL of Milli-Q water at a temperature of 50 °C and sonicated for 30 min; the procedure was repeated twice. After that, rinsing was done using Milli-Q water and drying in an oven at 50 °C for 1 h. The regenerated β-FeOOH/polyamide composites were then reused for catalytic ozonation treatment processes.

Investigation for the leaching of iron into the treated water during application of the β-FeOOH/polymeric composites was done at pH 3, pH 7 and pH 10. At the end of each catalytic ozonation process, the treated water samples were drawn and the iron levels were determined using an atomic absorption spectrophotometer (AAS) (Perkin Elmer 3300, Germany), with the data collected using AA WinLab Analyst software.

Toxicity studies

A toxicity bioassay was used to evaluate the possible associated ecological risk of the wastewater remediated with the polymeric nanocomposites. The analytical set-up included blank (control samples) and water samples after the remediation processes. Water flea (*Daphnia magna*), an aquatic crustacean, which is a primary consumer and a significant component of zooplankters in the ecosystem was used to assess toxicity. The acute toxicity testing was carried out at 24 h and 48 h inhibition of the mobility of the *D. magna* (ISO 6341), with a samples dilution percentile of 100, 50, 25, 12.5 and 6.25 in each case. The experimental data obtained were analysed using Toxrat Professional 3.2® for the determination of the statistical significance.

Results and discussion

Characterisation of β-FeOOH nanoparticles and its polymeric composite

TEM image of β-FeOOH (Fig. 2a) showed rod-like shaped nanoparticles with an average diameter and length of 5 nm and 15 nm, respectively. The ultra-small nanoparticles were well dispersed, with a d-spacing; 7.62 Å obtained from the selected area diffraction (Fig. 2b). The EDS spectrum (Fig. 3) shows the elemental analysis to be 47.01%, 43.75% and 9.24% for iron, oxygen, and chlorine, respectively. The chlorine peaks in the spectrum and the elemental percentage obtained suggest its presence in the hollandite channels of β-FeOOH [57], possibly offering stability to the tetragonal structure of the nanoparticles [58]. The captured TEM image for the 1.25 wt% β-FeOOH/polyamide composite (Fig. 4), shows evidence of the polymer matrix's embedded nanomaterials. Rod-like shapes distinctive of β-FeOOH nanoparticles are present and can be seen in the composite. The SEM image (SI Fig. 1) for the β-FeOOH shows the characteristic surface of a mesoporous material and supports the possible tunnel-like channels found in the nanoparticles [59].

The FTIR for the β-FeOOH nanoparticles, polyamide and the 1.25 wt% β-FeOOH/polyamide composite captured within 4000–400 cm^{-1} is presented in Fig. 5a. The β-FeOOH nanoparticles showed characteristic absorption peaks at wavelengths of 3339 cm^{-1} and 1624 cm^{-1} for O–H vibrations of absorbed water molecules [26]. Additionally, FTIR bands due to the vibration modes of the FeO_6 coordination octahedron were observed at wavelengths of 847 cm^{-1} and 651 cm^{-1} [60]. The FTIR spectrum for the polyamide is distinctive for the material, with some prominent peaks, which include the stretching and bending vibrations of hydrogen bonds in amide II occurring at 3324 cm^{-1} and 1536 cm^{-1}. A bending vibration in the same bond of amide in mode I correspond to the intense band at 1635 cm^{-1}, and this band overlaps the carbonyl group (-CO-) band located in the same region. The observed bands at 683 $cm^{-1}$and 574 cm^{-1} are assigned to the twisting vibrational bands of hydrogen in modes I and II of amide, respectively. The band at 3086 cm^{-1} represents the intramolecular bond that occurred between the amide and the carbonyl group (-$CONH_2$-) in the polyamide, while the doublet band at 2933 and 2866 corresponds to the vibrational symmetrical and asymmetrical stretching of the –CH_2 and –CH_3 groups, respectively [37]. The FTIR spectrum for the polymeric nanocomposite was similar to that of the pure polyamide with shift and decreased in the intensity of the band at 3086 cm^{-1}, representing the –$CONH_2$- intramolecular

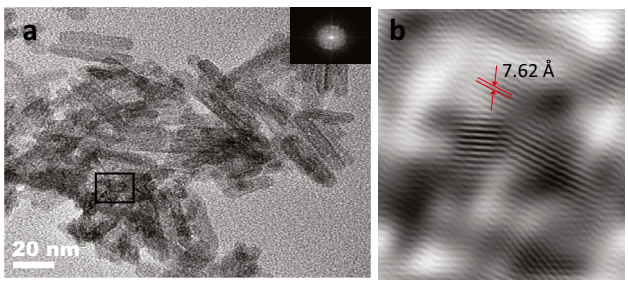

Fig. 2 (**a**) TEM images of β-FeOOH nanorods (insert: SAED patterns of the nanorods) and (**b**) D-spacing for the β-FeOOH nanoparticles

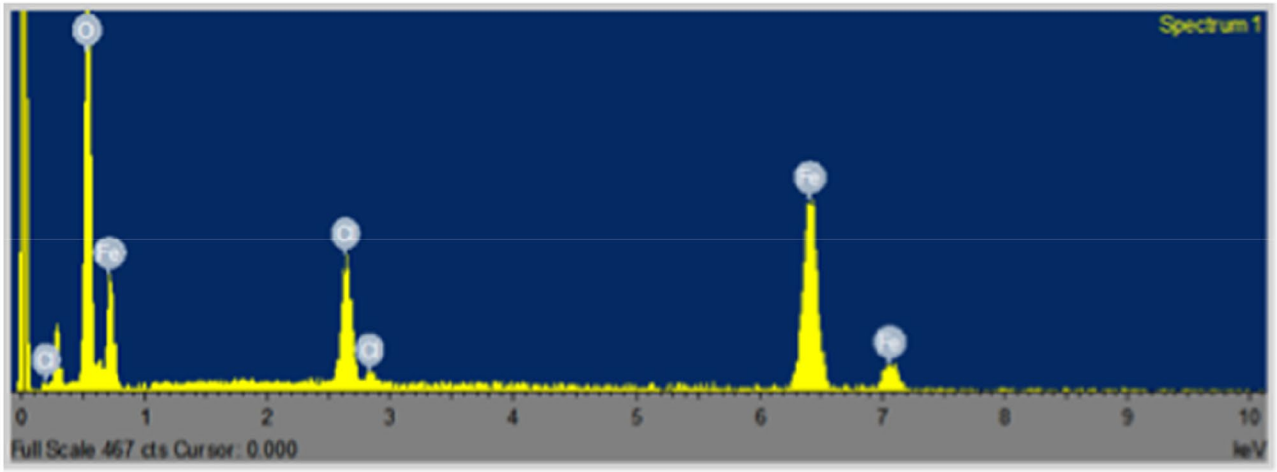

Fig. 3 EDS spectrum of the β-FeOOH showing the elemental atoms (Fe and O) and Cl^- atoms present inside the tunnels

bonds. The incorporated β-FeOOH nanoparticles utilising these same positions as coordination points in the polymer matrix may probably be the reason for the observed phenomenon. The nitrogen adsorption–desorption isotherm presented in Fig. 5b shows type IV with H1 hysteresis loops associated with mesoporous materials [61]. The Brunauer-Emmet-Teller (BET) surface area of the β-FeOOH nanoparticles was 154.34 $m^2\ g^{-1}$, while the Barrett-Joyner-Halender (BJH) pore volume and pore size was 0.32 $cm^3\ g^{-1}$ and 69.32 Å, respectively.

The X-ray diffraction patterns obtained for the β-FeOOH nanoparticles are a characteristic match, corresponding to the diffraction peaks of the nanomaterial (JCPDS 34–1266); Fig. 5c. The observed weak and broad peaks are indicative of the minute crystalline sizes, ranging in the nanometre scale, of the nanoparticles [62]. Also, the more intense (211) peak (compared to the 310) in the nanomaterial is indicative

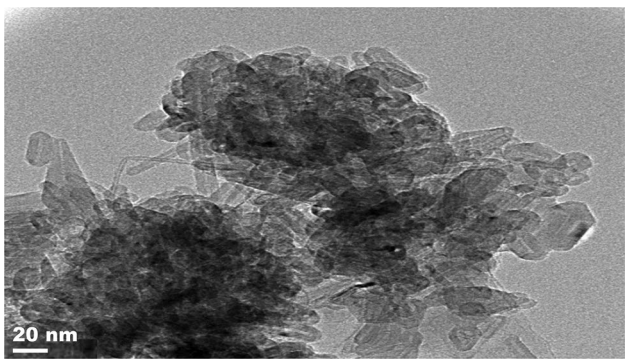

Fig. 4 TEM image of 1.25 wt% β-FeOOH/polyamide composite with visible nanorods orientation in the composite matrix

of the prevalence of the rod-like shape of the crystals [63], as confirmed by the TEM spectrum in Fig. 2a. The XRD patterns for polyamide are well-matched with several experimental patterns found in the literature [37, 43], showing the two characteristic crystallographic forms- α monoclinic and γ pseudo-hexagonal [64]. The α-phase of the XRD pattern of the diffraction peak can be identified at approximately $2\theta = 24.7°$, while the γ-phase was observed at 20.5° and 22°. The difference in the hydrogen bonds orientations is mainly responsible for the different polyamide polymorphs, with the γ pseudo-hexagonal phase being the product of parallel chain arrangement. In contrast, the anti-parallel chain arrangement forms the α monoclinic phase [37]. The phase composition of the 1.25 wt% β-FeOOH/polyamide composite largely resembles that of the polyamide, which forms its bulk. However, identifiable peaks of the β-FeOOH nanoparticles can be observed in the diffraction patterns of the composite at $2\theta = 27°$ and 35°. Also, the notable polyamide α monoclinic peak at $2\theta = 24.7°$ become broader, with a smaller peak at $2\theta = 23.5°$ observed before it, in the polymeric nanocomposite. This shows phase integration between the two starting materials with the β-FeOOH nanoparticles embedded into the polyamide matrix via the in situ polymerisation process.

Heterogeneous catalytic ozonation of 4-chlorophenol

Effect of β-FeOOH/polyamide PNC particle size

Field or large-scale application of polymeric nanocomposites is the ultimate goal, and this may be encouraged by the appropriate design and nature of the composites. Our

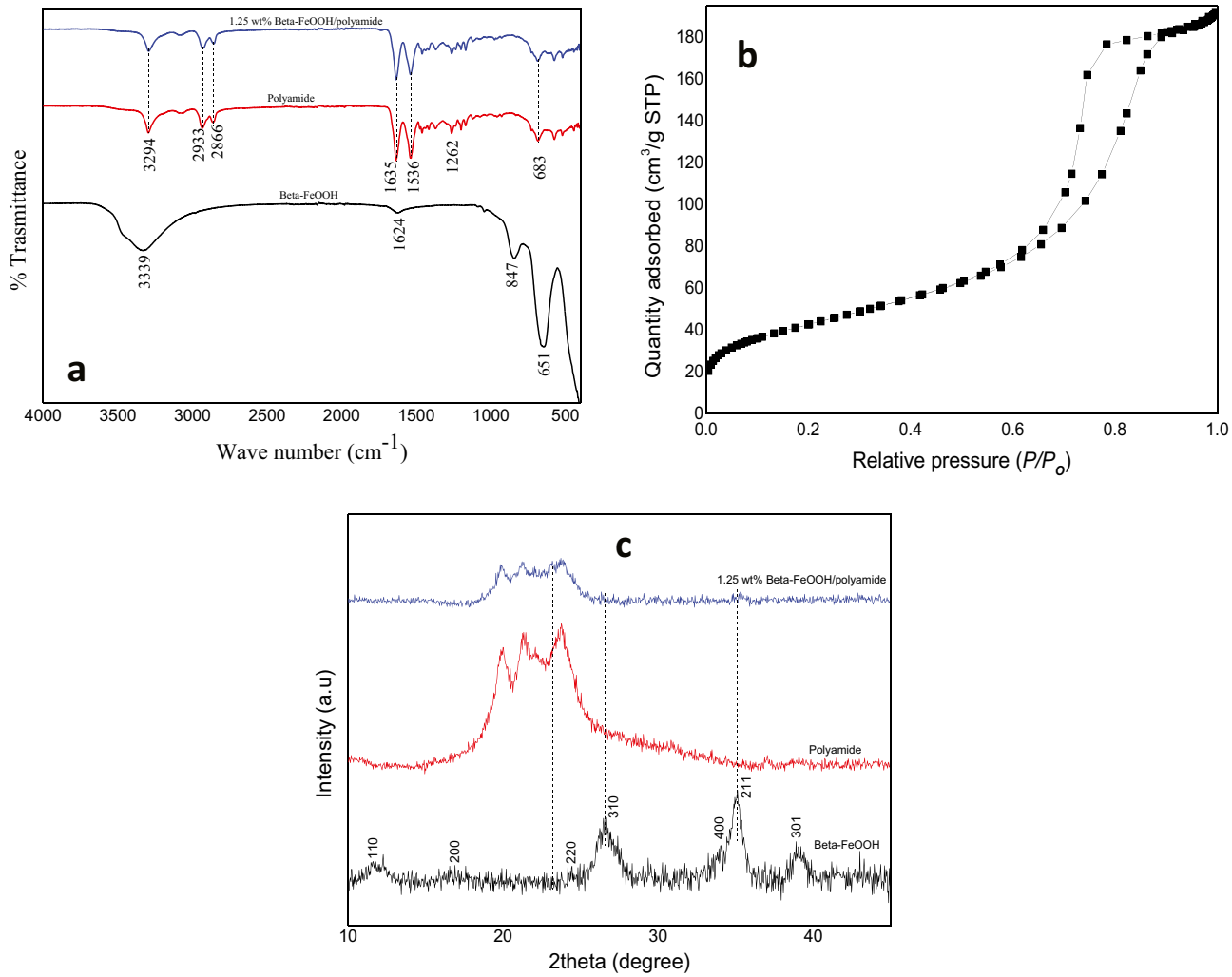

Fig. 5 (**a**) FTIR spectra of beta-FeOOH, polyamide and the 1.25 wt% β-FeOOH/polyamide composite, (**b**) nitrogen adsorption–desorption isotherm of β-FeOOH, and (**c**) XRD patterns of β-FeOOH nanoparticles, polyamide and the 1.25 wt% β-FeOOH/polyamide composite

approach to ensuring ease of field application was to optimise the size of the polymeric nanocomposites by grading them into size ranges that can be easily recovered as against using them in powdered form. As shown in Fig. 6a, three size grades of the 1.25 wt% β-FeOOH/polyamide were prepared and tested for their degradation capabilities. In their application for the catalytic ozonation of 2×10^{-3} M 4CP, it was revealed that the size range of 500–600 µm gave a better result, with 98.52% degradation recorded after 40 min. The other size ranges of 400–500 µm and 600–700 µm gave 92.81% and 85.84%, respectively. During the catalytic ozonation operations, which were accompanied by stirring, the 500–600 µm composites were suspended mainly in the region where the ozone was introduced into the analyte solution through the porous glass spout. The 600–700 µm were suspended below the entry point of ozone gas into the reactor vessel, while the 400–500 µm floated above the ozone introduction region. The achievement of optimum degradation requires the stability of the catalysts in suspension in and around the reaction zone, especially considering the half-life of the gas [26]. Composites with an average size of 500 – 600 µm were therefore selected for further studies.

Effect of β-FeOOH loading on polyamide and the reaction mechanism

The catalytic activity of the synthesised polymeric nanocomposites with different β-FeOOH loading (0.5, 0.75, 1.0 and 1.25 wt%) was evaluated in combination with ozone (Fig. 6b). There was a steady increase in the catalytic activity of the nanocomposites with increasing nanoparticles loading. The composite's 4CP removal efficiency of 98.52% was obtained with 1.25 wt% β-FeOOH loading after 40 min, while ozonation alone gave 62.94%. The incorporated β-FeOOH in combination with ozone produces HO^* due to surface reactions of the hydroxyl groups on β-FeOOH with

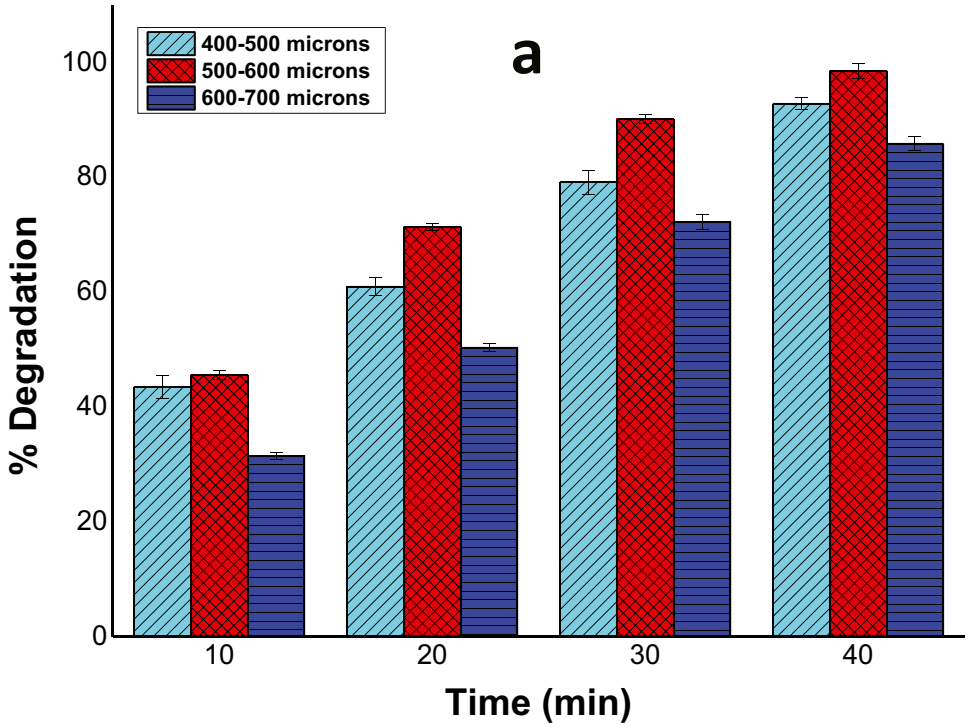

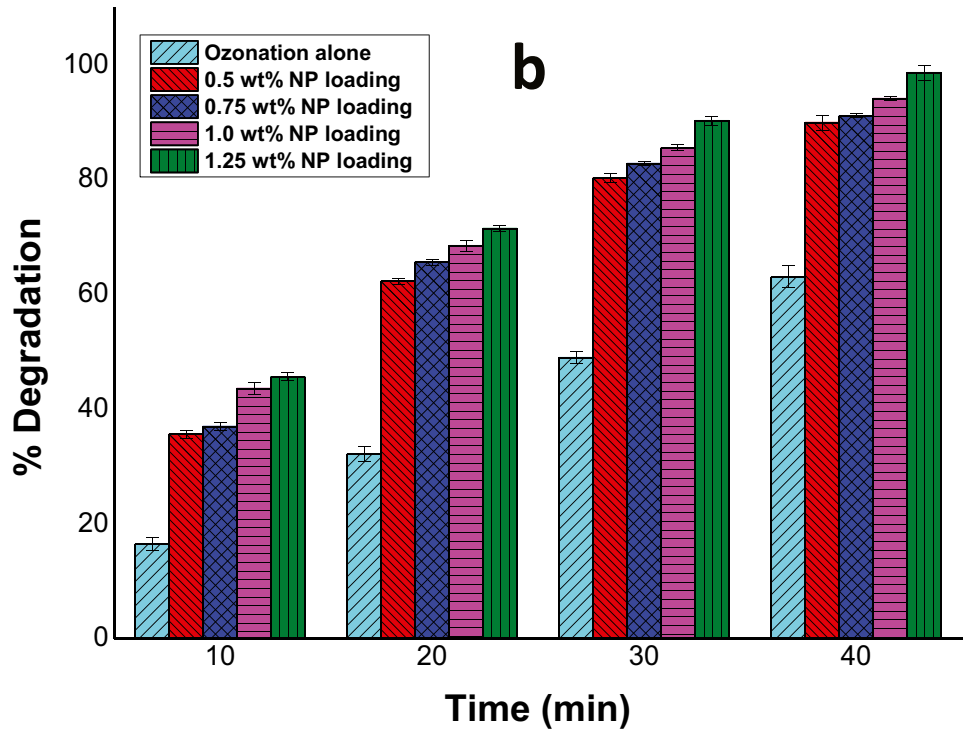

Fig. 6 (**a**) Catalytic ozonation degradation of 2×10^{-3} M 4CP using different size ranges of 1.25 wt% β-FeOOH/polyamide, (**b**) Degradation efficiency of the polymeric nanocomposites with different β-FeOOH loading

ozone [65, 66]. The introduction of metal oxides into water brings about a strong adsorption of water molecules [25, 67]; making the hydroxyl groups act like Brønsted acid sites and catalytic centres of the catalyst [68]. Ozone is unstable in water due to its high reactivity and can undergo electrophilic, nucleophilic or dipole reactions [66]. Ozone molecules undergo reactions with the Brønsted acid ($-OH_2^+$) formed on the surface hydroxyl groups present in the β-FeOOH nanoparticles. Therefore, Eqs. (3)–(7), supported by the literature above, is proposed as the probable reaction mechanism for the hydroxyl radical generation in this system. The generated hydroxyl radicals oxidise the 4CP adsorbed on the polymeric

nanocomposites or diffuses into the solution to oxidise the 4CP moieties present there [69]. Equation (7) proposes the stabilisation of the catalyst by the transfer of surface radicals to a hydroxyl group. The proposed mechanism for generating hydroxyl radical and degradation of the 4CP pollutant is shown in Fig. 7. The 4CP degradation has been reported to proceed via three primary, intermediate routes: catechol, 4- chlorocatechol and hydroquinone [70, 71].

$$FeO - OH + H_2O \rightarrow FeO - OH_2^+ + OH^- \quad (3)$$

$$FeO - OH_2^+ + O_3 \rightarrow FeO - OH^{\cdot +} + HO_3^{\cdot} \quad (4)$$

$$HO_3^{\cdot} \rightarrow HO^{\cdot} + O_2 \quad (5)$$

$$FeO - OH^{\cdot +} + H_2O \rightarrow FeO - OH_2^+ + HO^{\cdot} \quad (6)$$

$$FeO - OH^{\cdot +} + OH^- \rightarrow FeO - OH + HO^{\cdot} \quad (7)$$

Effect of hydroxyl radical scavenger in β-FeOOH/polyamide PNC reactions

To confirm the involvement of the HO^* in the degradation process of the analyte, methanol, a HO^* scavenger (with a rate constant as high as $9.6 \times 10^9\ M^{-1}\ S^{-1}$) was utilised in a ratio of 1:50 (4CP and methanol). The result, obtained by ozonation alone and the catalytic ozonation process, indicate that the 4CP degradation was majorly through the oxidative action of the HO^*. The degradation efficiency of 4CP was significantly reduced to 25.64% as compared to 62.94% and 98.52% for ozonation and the catalysed ozonation reactions, respectively (Fig. 8). The marked difference is accounted for by considering that most ozone molecules infused into the analyte solution are converted into HO^* in the catalysed reaction, thereby reducing their availability to degrade 4CP directly. Moreover, the generated HO^* are readily scavenged by the methanol, making them unavailable for the degradation of 4CP. In a similar heterogeneous catalytic process reported by Liu et al. [72], the degradation efficiency was reduced to zero when methanol was added to the FeO(OH)-reduced graphene oxide/H_2O_2/visible light system for 4CP removal.

Additionally, catalyst adsorption capability enhances the degradation efficiency of the contaminant, as their increasing adsorption on the surface of the catalyst gives higher efficiency [73, 74]. A preliminary test showed that the nanocomposites adsorb 21% of the 2×10^{-3} M 4CP solution after equilibrating for 60 min. Rapid migration of organic to composites surfaces, followed by oxidation by generated surface radicals, may contribute to the high oxidative degradation efficiency recorded during the catalytic ozonation process. The FTIR spectrum of the spent polymeric nanocomposites after six cycles of use (Fig. 9) was essentially the same, except for the changes in the intensities of the polymer characteristic absorption peaks- the amide II bending and stretching hydrogen bonds, the amide doublet band and the amide I bending vibrations. These changes did not significantly affect the catalytic property of the composite

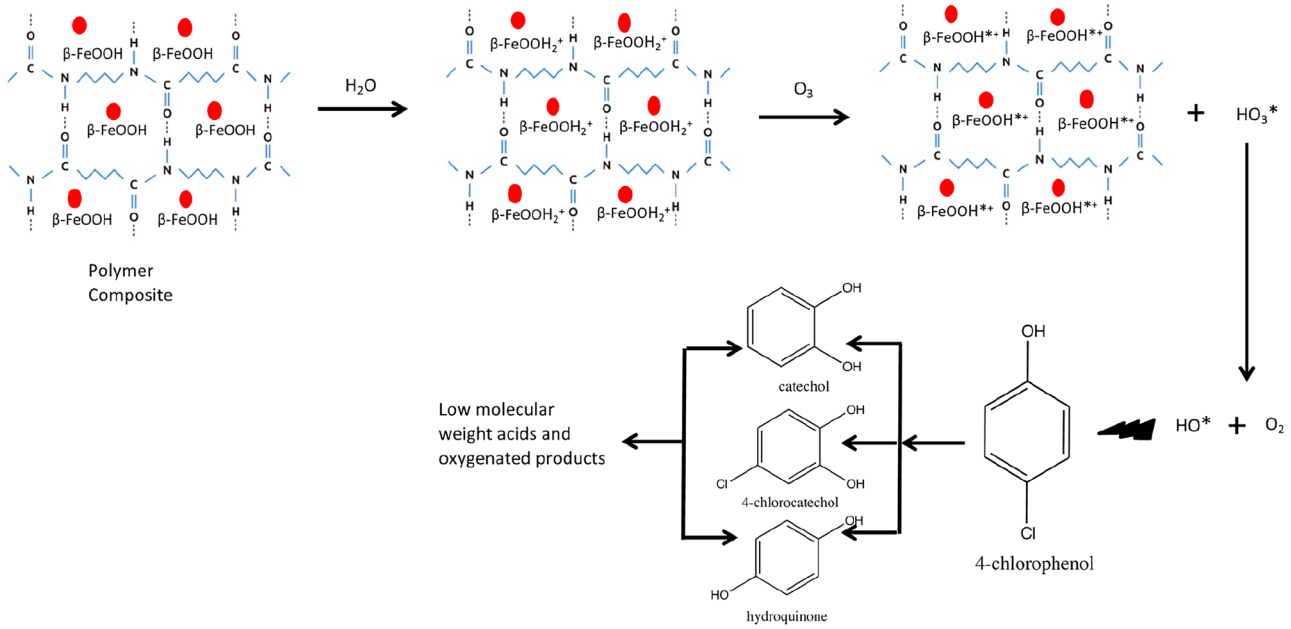

Fig. 7 The proposed mechanism for the generation of the hydroxyl radical and degradation of the 4CP pollutant

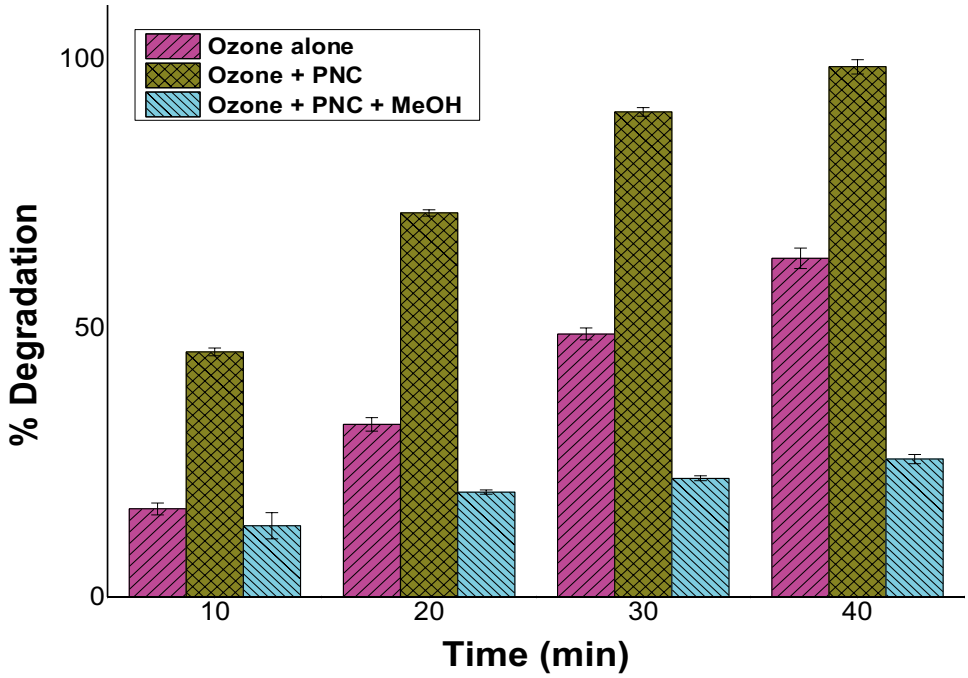

Fig. 8 Hydroxyl radicals scavenging effects of methanol in β-FeOOH/polyamide PNC reactions

as the degradation efficiency dropped by only 0.22% on the sixth reuse cycle. Furthermore, the solutions obtained from the regeneration of the polymeric nanocomposites between each reuse cycle were analysed to check for the presence of 4CP. The regeneration solutions did not show the presence of 4CP, suggesting that the surface adsorption of 4CP only aided its degradation, while the effective removal was by catalytic oxidation.

Effect of initial pH on β-FeOOH/polyamide PNC reactions

The pH of wastewaters undergoing remediation plays a critical role in the overall treatment output. The overall higher degradation efficiency of the 4CP was recorded at initial pH 10 with 96.01% removal after 30 min, compared to the 90.16% and 83.56% obtained for pH 7 and 3 as shown Fig. 10a. This trend is well supported by the literature as

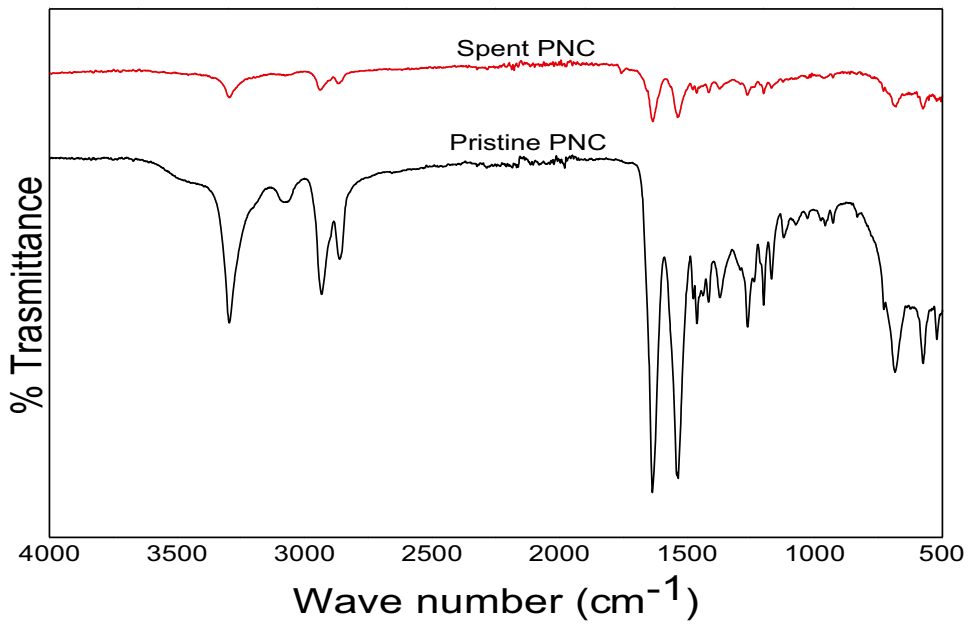

Fig. 9 FTIR spectra of pristine and spent polymeric nanocomposites after six reuse cycles

alkaline conditions lead to more efficient removal of 4CP [75] due to more HO^* radicals production in the solutions. The degradation rate of the 4CP solution with different initial pH values was evaluated using the pseudo-first-order reaction kinetics, and the duration was limited to 30 min due to the formation of intermediates (organic acids) that lowered the pH of the solutions [76]. The data presented in Fig. 10b shows that the reaction rate constant (ƙ) increased with the increasing pH values. Values of 0.0645, 0.0665 and 0.1123 were obtained for pH 3, pH 7 and pH 10, respectively.

β-FeOOH/polyamide PNC for the remediation of organics in natural wastewater

The final deployment of fabricated functional PNCs will be to remediate wastewaters. Hence, we carried out investigative tests to ascertain the potential of the β-FeOOH/polyamide composites to degrade organics in natural wastewater. Wastewater obtained from a treatment plant in the Boland region of Western Cape, South Africa, was treated with ozone alone and ozone combined with the synthesised PNCs. SI Table S2 shows the water quality parameters measured onsite for the influent and effluent samples.

The COD and TOC levels of the influent sample (wastewater) were determined, with 628 mg L^{-1} and 102 mg L^{-1} recorded, respectively. The catalytic ozonation process effectively reduced the COD and TOC values of the water to 285 mg L^{-1} (54.62% removal) and 11 mg L^{-1} (89.22% removal) respectively, after 60 min. Corresponding values were 415 mg L^{-1} (33.92% removal) and 54 mg L^{-1} (47.06% removal) when only ozone was used (Fig. 11a, b). The higher removal efficiency obtained from the catalysed ozonation process highlighted the potential of the β-FeOOH/polyamide composite for its application for wastewater remediation.

Regeneration and reuse of β-FeOOH/polyamide PNC

The economic cost of any treatment method determines to a large extent its scale of application and sustainability. Using polymeric nanocomposites over several application cycles without a drastic decline in their efficiencies may lead to a viable alternative treatment option. In this study, the β-FeOOH/polyamide composites were used over six cycles without significantly declining its degradation ability. Complete degradation (100%) was obtained after 60 min when the pristine composite was applied to degrade 2×10^{-3} M 4CP via the catalytic ozonation process (Fig. 12). Subsequent reuse after the regeneration cycle gave 99.73% efficiency for the 6th reuse. The regeneration process contributed to the reactivation of the active sites, possibly due to weak interacting bonds (physisorption) which existed between the β-FeOOH/polyamide and the contaminant or its degradation products. These superficial bonds were easily broken by hot water, and the active sites consequently regenerated.

Leaching studies

A core objective of this research was to address the challenge of reductive dissolution of the β-FeOOH, as reported by Oputu et al. [26]. The AAS results obtained from the analysis of the treated water at pH 3, 7 and 10, showed no leaching activity for the nanocomposites. The polyamide matrix provided adequate support for the β-FeOOH nanoparticles and the leaching of iron eliminated. The in situ preparation route for the polymeric nanocomposite might have provided a well-blended composite, with the nanoparticles embedded into the polyamide matrix. Generally, in situ methods provide a uniform dispersion of nanoparticles in polymer matrices through enhanced interpenetrative networks which lead

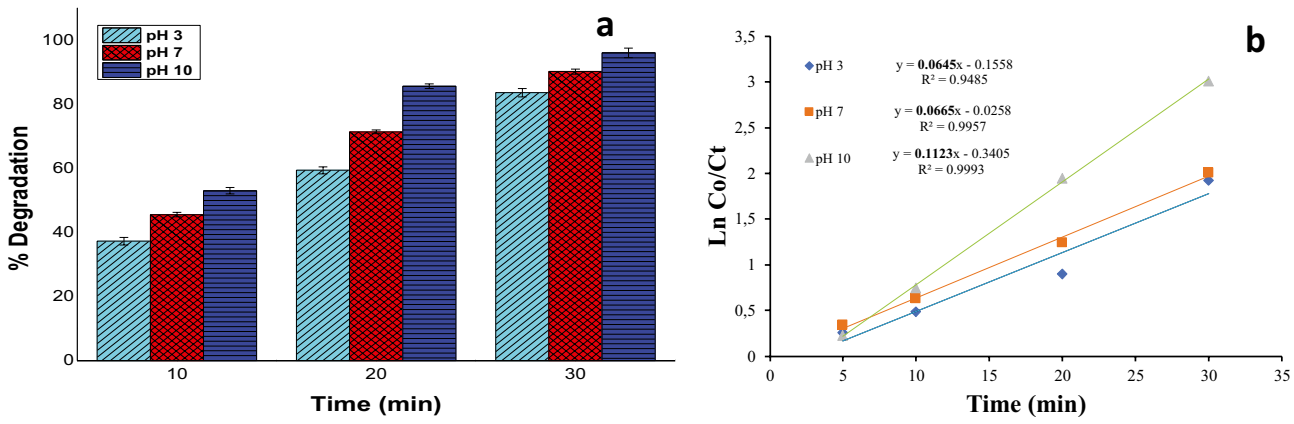

Fig. 10 (**a**) Degradation efficiency and (**b**) degradation rate (in bold) of 1.25 wt% β-FeOOH/polyamide utilised in combination with ozone for the degradation of 2×10^{-3} M 4CP at different initial pH

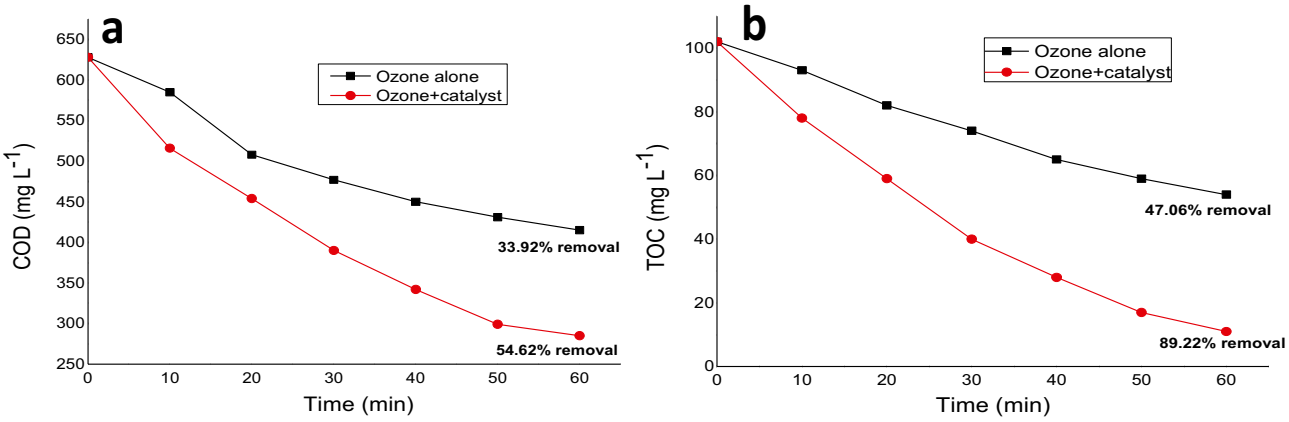

Fig. 11 (**a**) COD and (**b**) TOC removal from wastewater with ozone alone and catalysed ozonation

to higher compatibility between the constituents and stronger interfacial interactions [77]. However, as required for other water treatment materials such as activated carbon and ion exchange resins, the polymeric nanocomposites need to the rinsed before usage. Minimal Fe levels of 0.2296 and 0.0476 (Fig. 13) were obtained at pH 3 and 7 when the β-FeOOH/polyamide composites were utilised without prior rinsing (with Milli-Q water) before use. This suggested the presence of a few superficial β-FeOOH nanoparticles exposed after the composite post-polymerisation size grading. Additionally, the trend in the iron levels obtained for the 'un-rinsed' nanocomposites is consistent with the report of more reductive dissolution and Fe leaching at acidic pH [26].

Toxicity assay of treated wastewater

Toxicity assays are highly sensitive analytical tools to assess the environmental implications of pollutants and prove complementary to chemical assays for evaluating water quality [78, 79]. Toxicity data in literature often suggest that most wastewater treatment processes might not effectively eliminate wastewaters' toxicological effect patterns or compositions [78, 80]. The results of Daphnia acute toxicity testing are presented in Table 1. The results obtained show a general increase in the effective concentrations values, from LC_{10} to LC_{50} for both the 24 h and 48 h exposures, except in a few instances where no data was returned for the analysis.

The toxicity detection capacity in terms of the LOEC and NOEC gave a clear picture of the quality of the various water samples analysed. The 4CP contaminated water produced the most toxic effect against the test organisms with LOEC and NOEC values of > 6.250 and ≥ 6.250 percentile for 24 h and 48 h, respectively. From the chemical analysis, 4CP was completely degraded at 1 h of the catalysed ozonation process, and the degradation led to a reduction of the solution pH to ≈ 3 due to the breakdown of the analyte to

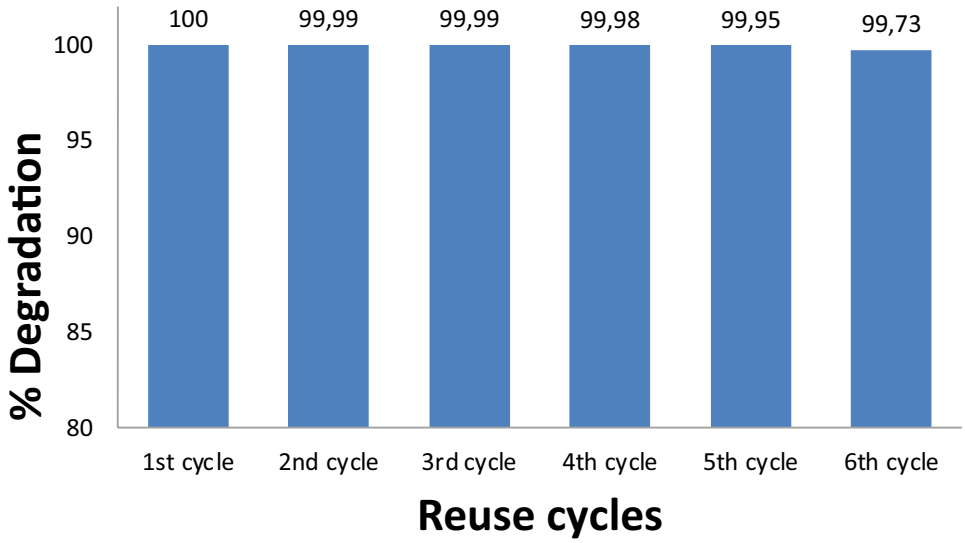

Fig. 12 Regeneration and reuse studies for β-FeOOH/polyamide composites in combination with ozone for 2×10^{-3} M 4CP degradation

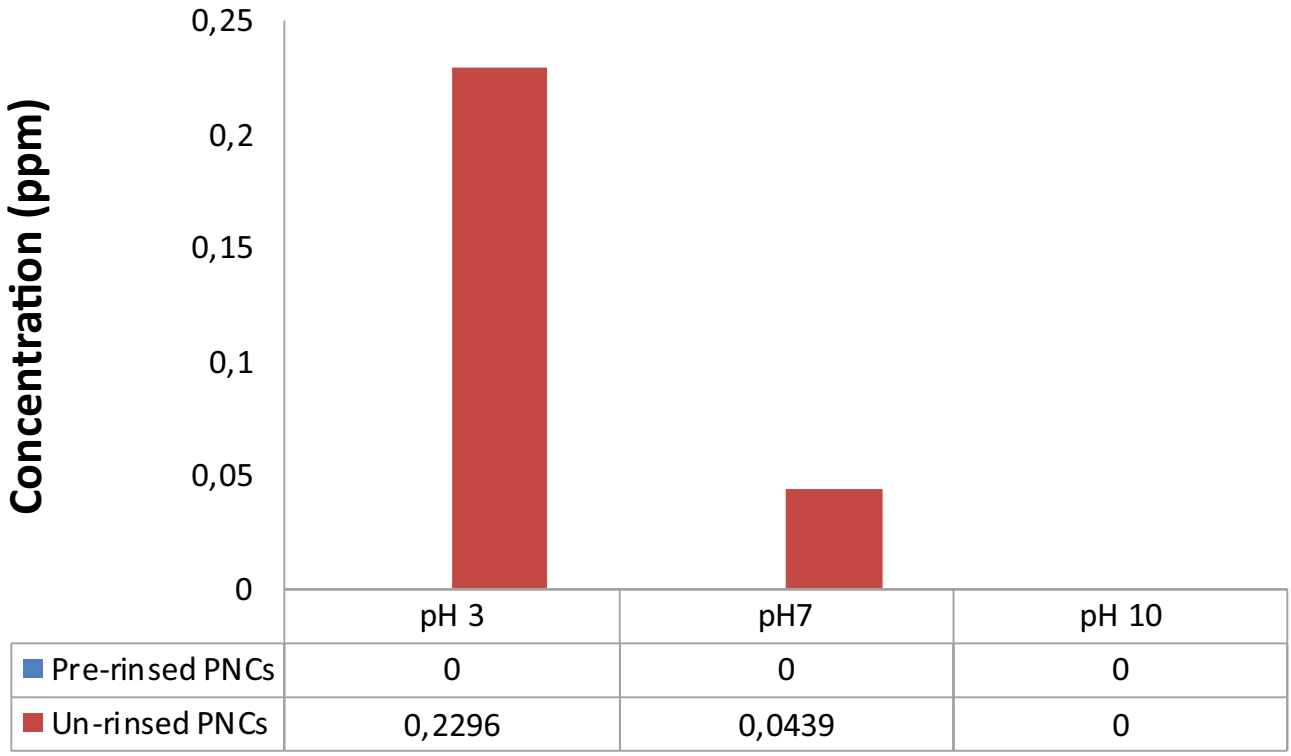

Fig. 13 Fe levels for the pre-rinsed and un-rinsed PNCs at different pH conditions

low molecular weight acids intermediates [70, 71]. Hence, the treated water at 1 h without pH adjustment was toxic to *D. magna* due to the acidic nature of the solution. The LOEC and NOEC values were both 6.250. Comparatively, the treated water at 1 h with adjusted pH (≈ 7) reduced mortality of the daphnids during the exposure period with the LOEC values of 50% and 12.5% observed for 24 h and 48 h exposures. The NOEC values were 100% and 25% for 24 h and 48 h, respectively.

Extension of the catalytic ozonation period for treatment efficiency comparison purposes was carried out at 1.5 h, 2 h and 3 h, respectively. The LOEC and NOEC values at 1.5 h were > 100% and ≥ 100% for 24 and 48 h respectively, indicating better water quality than the treatment carried out for 1 h. Conversely, the 2 h treatment period produced a decline in water quality. The LOEC value for the water sample was 100 and 25 percentiles for 24 h and 48 h, with NOEC values of 50 and 12.5 for 24 h and 48 h, respectively. Also, at

Table 1 Toxicity results for 4CP contaminated water and treated wastewater samples using *D. magna*

Water samples	Assay duration	LC_{10}	LC_{20}	LC_{50}	NOEC	LOEC
Treated wastewater at 1 h (pH = 7)	24 h	10.733	48.293	ND	100.0	50.0
	48 h	7.055	17.674	102.409	25.0	12.5
Treated wastewater at 1 h (unadjusted pH)	24 h	9.530	10.034	11.072	12.500	6.250
	48 h	8.206	8.425	8.861	12.500	6.250
Treated wastewater at 1.5 h (pH = 7)	24 h	ND	ND	ND	≥ 100.0	> 100.0
	48 h	37.387	ND	ND	≥ 100.0	> 100.0
Treated wastewater at 2 h (pH = 7)	24 h	22.999	40.367	118.417	50.0	100.0
	48 h	8.334	14.852	44.860	12.5	25.0
Treated wastewater at 3 h (pH = 7)	24 h	8.811	19.839	93.720	12.5	25.0
	48 h	ND	3.749	24.273	6.250	12.5
4CP contaminated water (0.002 M)	24 h	4.319	4.633	5.298	< 6.250	≤ 6.250
	48 h	3.561	3.875	4.556	< 6.250	≤ 6.250

LOEC Lowest observed effect concentration, *NOEC* No observed effect concentration, *LC* Effective concentration for xx% reduction, *95%-CL* 95% Confidence limits, *ND* not determined due to mathematical reasons or inappropriate data

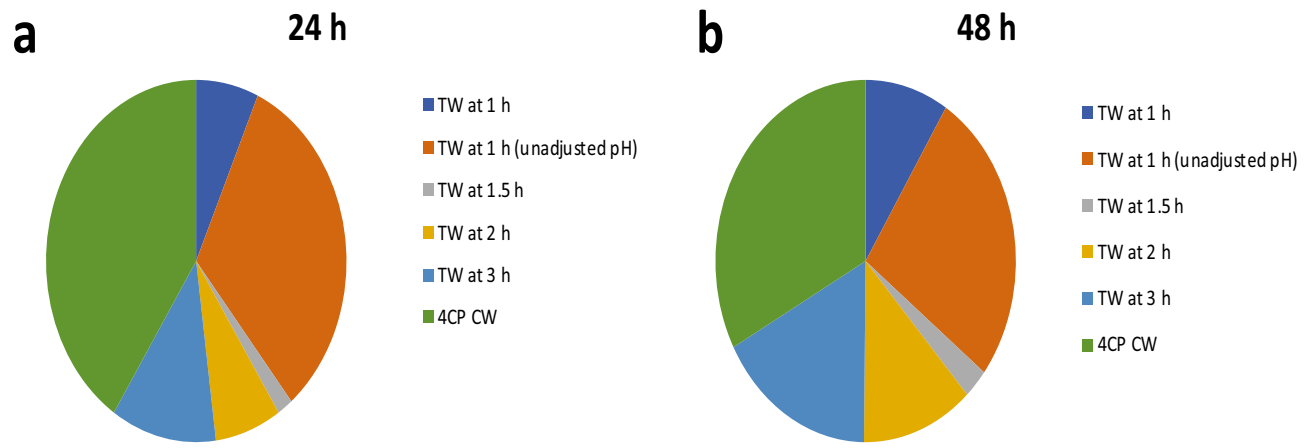

Fig. 14 Cumulative immobility analysis of the *D. magna* for the different water samples at (**a**) 24 h and (**b**) 48 h

the 3 h treatment duration, the LOEC further reduced to 25 and 12.5, while the NOEC was 12.5 and 6.250 for 24 h and 48 h, respectively. The indicative decline in the water quality after 1.5 h suggests excess ozone in the solution. Dehghani et al. [81] gave this assertion in a similar nano-catalysed process where increased toxicity was observed with time. The excessive hydrogen peroxide in solution at the extended time intervals was the adduced reason for the trend. The presence of excess ozone in water systems is a potential risk to aquatic organisms, especially the microorganisms [82]. Graphical representation of the cumulative immobility data of the *D. magna* for the different water samples at 24 h and 48 h are given in Fig. 14a, b. The acute immobilisation analysis supports the trend discussed above for LOEC and NOEC. The results confirmed the presence of toxic intermediates despite the complete degradation of the 4CP in the 1 h treated samples. After the complete degradation of the parent analyte, the treatment period should be extended for the complete removal of intermediates formed. Therefore, toxicity assays are important complementary tools with chemical analyses of water and wastewaters.

Future outlook and recommendation

In the last decade, there have been numerous investigations to synthesise plethora of nanoparticles and study their capacity to be used for water treatment purposes. These quests have produced many outputs of varying viability. However, a paradigm shift is now being established to incorporate the safe use of nanomaterials as a significant consideration in nano-based water treatment processes. This arises from the potential deposition of these nanomaterials in the water systems and the probable adverse effect that they may cause. Our study, taking this critical view into account, sought to use the polymer support to perform a dual role by helping to prevent the leaching/dissolution of the β-FeOOH nanoparticles during ozonation and to prevent the loss of catalyst. A critical point in nanomaterials applications is preventing catalyst loss during water treatment processes and their potential deposition in the environment. The use of appropriate matrices, such as polymers, can engender the development of this technology. Furthermore, a conscious effort to ascertain the quality of the treated water should be incorporated into emerging research in this area, as the perceived removal or degradation of the pollutant of interest alone may be of limited value. Toxicity assays are a sensitive analytical tool that can be used to assess the treated water quality as well as the environmental implications.

In general, most nano-based water treatment investigations are carried out mostly as lab-scale research. The full potential of the results can only be harnessed by deploying the nanomaterials in real or large scale operations. In this regard, new challenges may arise that were absent in the lab-scale experiments; however, it will create room for further research and improvement.

Conclusion

This investigation affirmed that polyamide can act as good support for β-FeOOH nanoparticles. The TEM image and XRD micrograph confirmed the incorporation of the nanoparticles in the polyamide matrix. The β-FeOOH/polyamide nanocomposites exhibited increasing degradation capability with increased nanoparticle loading. Significant increments in the degradation percentages were observed in the catalytic ozonation of 4CP in comparison to ozonation alone. Catalytic ozonation proved to be optimal at pH 10 due to the increased generation of the hydroxyl radicals in the solution. The COD and TOC values for natural wastewater were effectively reduced by 54.62% and 89.22% after 60 min by the polymeric nanocatalyst. The PNC showed excellent reuse

potential, with a minimal decrease in its degradation efficiency over six cycles. No iron leaching was observed during use in acidic, neutral and alkaline conditions. The toxicity assay gave excellent insight into the treated water quality. At the treatment duration of 1 h, when the 4CP was fully degraded as confirmed using LCMS-TOF, the treated water still exhibited a significant level of toxicity to the daphnids. The 4CP contaminated water treated for 1.5 h had better quality, with pH adjustment of the treated water found to be necessary to reduce the mortality of *D. magna*. The novel PNC gave promising remediation capability and proved effective for the degradation of 4CP in aqueous solutions. The use of the composites gave some operational advantages such as prevention of nanoparticles loss, ease of recovery and regeneration for reuse, and the subsequent safeguarding of our environment and the biota therein.

Supplementary information The online version contains supplementary material available at https://doi.org/10.1007/s10965-022-03007-4.

Acknowledgements The authors acknowledge the Cape Peninsula University of Technology, South Africa, for the provision of infrastructure for the study and financial support to the lead author through their Postgraduate Bursary Scheme. We also thank Ms Daniela Kucich for proofreading the manuscript.

Authors' contributions Conceptualisation: BOO, OSF; Methodology: MOA; Formal analysis and investigation: MOA, OP, OUO; Software: MOA, OP; Writing–original draft preparation: MOA; Writing–review and editing: OP, OUO; Resources: BOO, OSF; Supervision: BOO, OSF, DIO.

Availability of data and materials All data generated or analysed during this study are included in this published article and its supplementary information files.

Declarations

Ethics approval and consent to participate Not Applicable.

Consent for publication Not Applicable.

Competing interests The authors declare that they have no competing interests.

References

1. Wang S, Zhu Z, He J, Yue X, Pan J, Wang Z (2018) Steroidal and phenolic endocrine disrupting chemicals (EDCs) in surface water of Bahe River, China: distribution, bioaccumulation, risk assessment and estrogenic effect on *Hemiculter leucisculus*. Environ Pollut 243:103–114. https://doi.org/10.1016/j.envpol.2018.08.063
2. Zhou X, Yang Z, Luo Z, Li H, Chen G (2019) Endocrine disrupting chemicals in wild freshwater fishes: species, tissues, sizes and human health risks. Environ Pollut 244:462–468. https://doi.org/10.1016/j.envpol.2018.10.026
3. Michałowicz J, Duda W (2007) Phenols- sources and toxicity. Pol J Environ Stud 16(3):347–362
4. Park JS, Brown MT, Han T (2012) Phenol toxicity to the aquatic macrophyte *Lemna paucicostata*. Aquat Toxicol 106–107:182–188. https://doi.org/10.1016/j.aquatox.2011.10.004
5. Erler C, Novak J (2010) Bisphenol a exposure: human risk and health policy. J Pediatr Nurs 25:400–407. https://doi.org/10.1016/j.pedn.2009.05.006
6. Jimenez-Becerril J, Martinez-Hernandez A, Granados-Correa F, Zavala Arce RE (2013) Methylene blue and 4-chlorophenol photodegradation using Gamma-irradiated titanium oxide. J Chem Soc Pak 35:23–26
7. Kumar A, Guo C, Sharma G, Pathania D, Naushad M, Kalia S, Dhiman P (2016) Magnetically recoverable ZrO_2/Fe_3O_4/chitosan nanomaterials for enhanced sunlight driven photoreduction of carcinogenic Cr(VI) and dechlorination and mineralization of 4-chlorophenol from simulated waste water. RSC Adv 6:13251–13263. https://doi.org/10.1039/C5RA23372K
8. Haddadi A, Shavandi M (2013) Biodegradation of phenol in hypersaline conditions by *Halomonas sp.* strain PH2-2 isolated from saline soil. Int Biodeterior Biodegrad 85:29–34. https://doi.org/10.1016/j.ibiod.2013.06.005
9. Lim J-W, Lim P-E, Seng C-E, Adnan R (2013) Simultaneous 4-chlorophenol and nitrogen removal in moving bed sequencing batch reactors packed with polyurethane foam cubes of various sizes. Bioresour Technol 129:485–494. https://doi.org/10.1016/j.biortech.2012.11.111
10. Nalbur BE, Alkan U (2007) The inhibitory effects of 2-CP and 2, 4-DCP containing effluents on sequencing batch reactors. Int Biodeterior Biodegrad 60:178–188. https://doi.org/10.1016/j.ibiod.2007.03.001
11. Jianping W, Hongmei L, Jing B, Jiang Y (2006) Biodegradation of 4-chlorophenol by *Candida albicans* PDY-07 under anaerobic conditions. Chin J Chem Eng 14:790–795. https://doi.org/10.1016/S1004-9541(07)60013-5
12. Giebner S, Ostermann S, Straskraba S, Oetken M, Oehlmann J, Wagner M (2018) Effectivity of advanced wastewater treatment: reduction of in vitro endocrine activity and mutagenicity but not of in vivo reproductive toxicity. Environ Sci Pollut Res 25:3965–3976. https://doi.org/10.1007/s11356-016-7540-1
13. Covinich LG, Bengoechea DI, Fenoglio RJ, Area MC (2014) Advanced oxidation processes for wastewater treatment in the pulp and paper industry: a review. Amer J Environ Eng 4:56–70. https://doi.org/10.5923/j.ajee.20140403.03
14. Litter M, Quici N (2010) Photochemical advanced oxidation processes for water and wastewater treatment. Recent Pat Eng 4:217–241. https://doi.org/10.2174/187221210794578574
15. Huang X, Wang R, Jiao T, Zou G, Zhan F, Yin J, Zhang L, Zhou J, Peng Q (2019) Facile preparation of hierarchical AgNP-loaded MXene/Fe_3O_4/polymer nanocomposites by electrospinning with enhanced catalytic performance for wastewater treatment. ACS Omega 4:1897–1906. https://doi.org/10.1021/acsomega.8b03615
16. Luan H, Teychene B, Huang H (2019) Efficient removal of As(III) by Cu nanoparticles intercalated in carbon nanotube membranes for drinking water treatment. Chem Eng J 355:341–350. https://doi.org/10.1016/j.cej.2018.08.104
17. Rizvi MA, Moosvi SK, Jan T, Bashir S, Kumar P, Roos WD, Swart HC (2019) Dielectric, magnetic and photocatalytic activity of polypyrrole/Prussian red nanocomposite for waste water treatment applications. Polymer 163:1–12. https://doi.org/10.1016/j.polymer.2018.12.044
18. Peydayesh M, Mohammadi T, Bakhtiari O (2018) Effective treatment of dye wastewater via positively charged TETA-MWCNT/PES hybrid nanofiltration membranes. Sep Purif Technol 194:488–502. https://doi.org/10.1016/j.seppur.2017.11.070

19. Kochameshki MG, Marjani A, Mahmoudian M, Farhadi K (2017) Grafting of diallyldimethylammonium chloride on graphene oxide by RAFT polymerization for modification of nanocomposite polysulfone membranes using in water treatment. Chem Eng J 309:206–221. https://doi.org/10.1016/j.cej.2016.10.008
20. El-Qanni A, Nassar NN, Vitale G, Hassan A (2016) Maghemite nanosorbcats for methylene blue adsorption and subsequent catalytic thermo-oxidative decomposition: computational modeling and thermodynamics studies. J Colloid Interface Sci 461:396–408. https://doi.org/10.1016/j.jcis.2015.09.041
21. Parlayici S, Eskizeybek V, Avcı A, Pehlivan E (2015) Removal of chromium (VI) using activated carbon-supported-functionalized carbon nanotubes. J Nanostructure Chem 5:255–263. https://doi.org/10.1007/s40097-015-0156-z
22. Xia S, Gu Z, Zhang J, Hermanowicz SW (2014) Removal of chloramphenicol from aqueous solution by nanoscale zero-valent iron particles. Chem Eng J 257:98–104. https://doi.org/10.1016/j.cej.2014.06.106
23. Cornell RM, Schwertmann U (2003) The iron oxides: structure, properties, reactions, occurrences and uses, 2nd edn. John Wiley & Sons, Weinheim, Germany
24. Ebrahim S, Shokry A, Ibrahim H, Soliman M (2016) Polyaniline/akaganéite nanocomposite for detoxification of noxious Cr(VI) from aquatic environment. J Polym Res 23:79–80. https://doi.org/10.1007/s10965-016-0977-6
25. Wang C, Li A, Shuang C (2018) The effect on ozone catalytic performance of prepared-FeOOH by different precursors. J Environ Manag 228:158–164. https://doi.org/10.1016/j.jenvman.2018.08.103
26. Oputu O, Chowdhury M, Nyamayaro K, Fatoki O, V. Fester V, (2015) Catalytic activities of ultra-small beta-FeOOH nanorods in ozonation of 4-chlorophenol. J Environ Sci 35:83–90. https://doi.org/10.1016/j.jes.2015.02.013
27. Obregón S, Barriga-Castro E, Mendoza-Reséndez R, Luna C (2016) Enhanced photocatalytic behavior of $BiVO_4$ through photoinduced charge transfer to amorphous β-FeOOH nanoparticles. Ceram Int 42:17773–17780. https://doi.org/10.1016/j.ceramint.2016.08.105
28. Oputu O, Chowdhury M, Nyamayaro K, Cummings F, Fester V, Fatoki O (2015) A novel β-FeOOH/NiO composite material as a potential catalyst for catalytic ozonation degradation of 4-chlorophenol. RSC Adv 5:59513–59521. https://doi.org/10.1039/C5RA09177B
29. Chowdhury M, Ntiribinyange M, Nyamayaro K, Fester V (2015) Photocatalytic activities of ultra-small β-FeOOH and TiO_2 heterojunction structure under simulated solar irradiation. Mater Res Bull 68:133–141. https://doi.org/10.1016/j.materresbull.2015.03.044
30. Zhu T, Ong WL, Zhu L, Ho GW (2015) TiO_2 fibers supported β-FeOOH nanostructures as efficient visible light photocatalyst and room temperature sensor. Sci Rep 5:10601. https://doi.org/10.1038/srep10601
31. Xiao F, Li W, Fang L, Wang D (2016) Synthesis of akageneite (beta-FeOOH)/reduced graphene oxide nanocomposites for oxidative decomposition of 2-chlorophenol by Fenton-like reaction. J Hazard Mater 308:11–20. https://doi.org/10.1016/j.jhazmat.2016.01.011
32. Zheng Y, Zhang Z, Li C (2016) Beta-FeOOH-supported graphitic carbon nitride as an efficient visible light photocatalyst. J Mol Catal A Chem 423:463–471
33. Akharame MO, Fatoki OS, Opeolu BO (2019) Regeneration and reuse of polymeric nanocomposites in wastewater remediation: the future of economic water management. Polym Bull 76:647–681. https://doi.org/10.1007/s00289-018-2403-1
34. Akharame MO, Oputu OU, Pereao O, Fagbayigbo BO, Razanamahandry LC, Opeolu BO, Fatoki OS (2019) Nanostructured polymer composites for water remediation. In Gonçalve GAB, Marques P (ed) Nanostructured Materials for Treating Aquatic Pollution, Springer, Switzerland. https://doi.org/10.1007/978-3-030-33745-2_10
35. Qu X, Brame J, Li Q, Alvarez PJ (2012) Nanotechnology for a safe and sustainable water supply: enabling integrated water treatment and reuse. Acc Chem Res 46:834–843. https://doi.org/10.1021/ar300029v
36. Akharame MO, Fatoki OS, Opeolu BO, Olorunfemi DI, Oputu OU (2018) Polymeric Nanocomposites (PNCs) for wastewater remediation: an overview. Polym Plast Technol Eng 57:1801–1827. https://doi.org/10.1080/03602559.2018.1434666
37. Farias-Aguilar JC, Ramírez-Moreno MJ, Téllez-Jurado L, Balmori-Ramírez H (2014) Low pressure and low temperature synthesis of polyamide-6 (PA6) using Na^0 as catalyst. Mater Lett 136:388–392. https://doi.org/10.1016/j.matlet.2014.08.071
38. O'Neill A, Bakirtzis D, Dixon D (2014) Polyamide 6/Graphene composites: the effect of in situ polymerisation on the structure and properties of graphene oxide and reduced graphene oxide. Eur Polym J 59:353–362. https://doi.org/10.1016/j.eurpolymj.2014.07.038
39. Espeso J, Lozano AE, José G, de Abajo J (2006) Effect of substituents on the permeation properties of polyamide membranes. J Membr Sci 280:659–665. https://doi.org/10.1016/j.memsci.2006.02.023
40. Palabiyik M, Bahadur S (2000) Mechanical and tribological properties of polyamide 6 and high density polyethylene polyblends with and without compatibilizer. Wear 246:149–158. https://doi.org/10.1016/S0043-1648(00)00501-9
41. Basaleh AA, Al-Malack MH, Saleh TA (2019) Methylene blue removal using polyamide-vermiculite nanocomposites: kinetics, equilibrium and thermodynamic study. J Environ Chem Eng 7:103107. https://doi.org/10.1016/j.jece.2019.103107
42. Ali I, AL-Hammadi SA, Saleh TA (2018) Simultaneous sorption of dyes and toxic metals from waters using synthesized titania-incorporated polyamide. J Mol Liq 269:564–571. https://doi.org/10.1016/j.molliq.2018.08.081
43. Wang L, Fang M, Liu J, He J, Deng L, Li J, Lei J (2015) The influence of dispersed phases on polyamide/ZIF-8 nanofiltration membranes for dye removal from water. RSC Adv 5:50942–50954. https://doi.org/10.1039/C5RA06185G
44. Wang L, Fang M, Liu J, He J, Li J, Lei J (2015) Layer-by-layer fabrication of high-performance polyamide/ZIF-8 nanocomposite membrane for nanofiltration applications. ACS Appl Mater Interfaces 7:24082–24093. https://doi.org/10.1021/acsami.5b07128
45. Lombardi M, Palmero P, Sangermano M, Varesano A (2011) Electrospun polyamide-6 membranes containing titanium dioxide as photocatalyst. Polym Int 60:234–239. https://doi.org/10.1002/pi.2932
46. Özdilek C, Kazimierczak K, van der Beek D, Picken SJ (2004) Preparation and properties of polyamide-6-boehmite nanocomposites. Polymer 45:5207–5214. https://doi.org/10.1016/j.polymer.2004.05.029
47. Oh K, Kim H, Seo Y (2019) Effect of diamine addition on structural features and physical properties of polyamide 6 synthesized by anionic ring-opening polymerization of ε-caprolactam. ACS Omega 4:17117–17124. https://doi.org/10.1021/acsomega.9b01342
48. Dinari M, Mohammadnezhad G, Nabiyan A (2016) Preparation and characterization of nanocomposite materials based on polyamide-6 and modified ordered mesoporous silica KIT-6. J Appl Polym Sci 133:43098–43103. https://doi.org/10.1002/app.43098
49. Shokry A, El-Tahan A, Ibrahim H, Soliman M, Ebrahim S (2019) Polyaniline/akaganéite superparamagnetic nanocomposite for cadmium uptake from polluted water. Desalin Water Treat 171:205–215. https://doi.org/10.5004/dwt.2019.24835
50. Chowdhury MR, Fester V, Kale G, Cespedes O (2014) Hydrothermal precipitation of β-FeOOH nanostructure(s) in mixed solvent: study of their morphological and structural

evolution. J Nanoparticle Res 16:2412. https://doi.org/10.1007/s11051-014-2412-4
51. Coelho AA (2007) TOPAS-academic. Coelho Software, Brisbane, Australia
52. Chou M-S, Chang K-L (2007) Oxidation of aqueous dimethyl sulfoxide (DMSO) using UV, O_3, and UV/O_3. Ozone Sci Eng 29:391–397. https://doi.org/10.1080/01919510701573418
53. Urbano VR, Maniero MG, Pérez-Moya M, Guimarães JR (2017) Influence of pH and ozone dose on sulfaquinoxaline ozonation. J Environ Manag 195:224–231. https://doi.org/10.1016/j.jenvman.2016.08.019
54. van Leeuwen J (2015) Proposed OS&E requirement: measuring ozone dosage. Ozone Sci Eng 37:191–192. https://doi.org/10.1080/01919512.2015.1006467
55. Li F, Du P, Liu W, Li X, Ji H, Duan J, Zhao D (2018) Hydrothermal synthesis of graphene grafted titania/titanate nanosheets for photocatalytic degradation of 4-chlorophenol: solar-light-driven photocatalytic activity and computational chemistry analysis. Chem Eng J 331:685–694. https://doi.org/10.1016/j.cej.2017.09.036
56. Liu W, Ni J, Yin X (2014) Synergy of photocatalysis and adsorption for simultaneous removal of Cr(VI) and Cr(III) with TiO_2 and titanate nanotubes. Water Res 53:12–25. https://doi.org/10.1016/j.watres.2013.12.043
57. Song X, Boily J-H (2012) Competitive ligand exchange on akaganéite surfaces enriches bulk chloride loadings. J Colloid Interface Sci 376:331–333. https://doi.org/10.1016/j.jcis.2012.03.006
58. Yue J, Jiang X, Yu A (2011) Experimental and theoretical study on the β-FeOOH nanorods: growth and conversion. J Nanoparticle Res 13:3961–3974. https://doi.org/10.1007/s11051-011-0320-4
59. Yuan Z-Y, Ren T-Z, Su B-L (2004) Surfactant mediated nanoparticle assembly of catalytic mesoporous crystalline iron oxide materials. Catal Today 93:743–750. https://doi.org/10.1016/j.cattod.2004.06.092
60. Xu Z, Zhang M, Wu J, Liang J, Zhou L, Lǔ B (2013) Visible light-degradation of azo dye methyl orange using TiO_2/β-FeOOH as a heterogeneous photo-Fenton-like catalyst. Water Sci Technol 68:2178–2185. https://doi.org/10.2166/wst.2013.475
61. Kruk M, Jaroniec M (2001) Gas adsorption characterization of ordered organic− inorganic nanocomposite materials. Chem Mater 13:3169–3183. https://doi.org/10.1021/cm0101069
62. Yuan Z-Y, Su B-L (2003) Surfactant-assisted nanoparticle assembly of mesoporous β-FeOOH (akaganeite). Chem Phys Lett 381:710–714. https://doi.org/10.1016/j.cplett.2003.10.033
63. Schwertmann U, Cornell R (1991) Iron oxides in the Laboratory: preparation and characterization. Wiley VCH Verlag GmbH, Weinheim
64. Khanna Y, Kuhn W (1997) Measurement of crystalline index in nylons by DSC: complexities and recommendations. J Polym Sci B Polym Phys 35:2219–2231. https://doi.org/10.1002/(SICI)1099-0488(199710)35:14%3C2219::AID-POLB3%3E3.0.CO;2-R
65. Zhao L, Sun Z, Ma J, Liu H (2009) Enhancement mechanism of heterogeneous catalytic ozonation by cordierite-supported copper for the degradation of nitrobenzene in aqueous solution. Environ Sci Technol 43:2047–2053. https://doi.org/10.1021/es803125h
66. Kasprzyk-Hordern B, Ziółek M, Nawrocki J (2003) Catalytic ozonation and methods of enhancing molecular ozone reactions in water treatment. Appl Catal B Environ 46:639–669. https://doi.org/10.1016/S0926-3373(03)00326-6
67. Yang L, Hu C, Nie Y, Qu J (2010) Surface acidity and reactivity of β-FeOOH/Al_2O_3 for pharmaceuticals degradation with ozone: in situ ATR-FTIR studies. Appl Catal B Environ 97:340–346. https://doi.org/10.1016/j.apcatb.2010.04.014
68. Yang L, Hu C, Nie Y, Qu J (2009) Catalytic ozonation of selected pharmaceuticals over mesoporous alumina-supported manganese oxide. Environ Sci Technol 43:2525–2529. https://doi.org/10.1021/es803253c
69. Sui M, Sheng L, Lu K, Tian F (2010) FeOOH catalytic ozonation of oxalic acid and the effect of phosphate binding on its catalytic activity. Appl Catal B Environ 96:94–100. https://doi.org/10.1016/j.apcatb.2010.02.005
70. Oputu OU, Fatoki OS, Opeolu BO, Akharame MO (2020) Degradation pathway of ozone oxidation of phenols and chlorophenols as followed by LC-MS-TOF. Ozone Sci Eng 42:294–318. https://doi.org/10.1080/01919512.2019.1660617
71. Akharame MO, Fatoki OS, Opeolu BO, Olorunfemi DI, Oputu OU (2020) Comparative time-based intermediates study of ozone oxidation of 4-chloro-and 4-nitrophenols followed by LCMS-TOF. J Environ Sci Health A 55:385–401. https://doi.org/10.1080/10934529.2019.1701340
72. Liu R, Xu Y, Chen B (2018) Self-assembled nano-FeO(OH)/reduced graphene oxide aerogel as a reusable catalyst for photo-Fenton degradation of phenolic organics. Environ Sci Technol 52:7043–7053. https://doi.org/10.1021/acs.est.8b01043
73. Sharma VK, McDonald TJ, Kim H, Garg VK (2015) Magnetic graphene–carbon nanotube iron nanocomposites as adsorbents and antibacterial agents for water purification. Adv Colloid Interface Sci 225:229–240. https://doi.org/10.1016/j.cis.2015.10.006
74. Ghanem AF, Badawy AA, Ismail N, Tian ZR, Rehim MA, Rabia A (2014) Photocatalytic activity of hyperbranched polyester/TiO_2 nanocomposites. Appl Catal A Gen 472:191–197. https://doi.org/10.1016/j.apcata.2013.12.023
75. Hirvonen A, Trapido M, Hentunen J, Tarhanen J (2000) Formation of hydroxylated and dimeric intermediates during oxidation of chlorinated phenols in aqueous solution. Chemosphere 41:1211–1218. https://doi.org/10.1016/S0045-6535(99)00548-2
76. García-Molina V, Lopez-Arias M, Florczyk M, Chamarro E, Esplugas S (2005) Wet peroxide oxidation of chlorophenols. Water Res 39:795–802. https://doi.org/10.1016/j.watres.2004.12.007
77. Kango S, Kalia S, Celli A, Njuguna J, Habibi Y, Kumar R (2013) Surface modification of inorganic nanoparticles for development of organic–inorganic nanocomposites—A review. Prog Polym Sci 38:1232–1261. https://doi.org/10.1016/j.progpolymsci.2013.02.003
78. Välitalo P, Massei R, Heiskanen I, Behnisch P, Brack W, Tindall AJ, Du Pasquier E, Küster E, Mikola A, Schulze T (2017) Effect-based assessment of toxicity removal during wastewater treatment. Water Res 126:153–163. https://doi.org/10.1016/j.watres.2017.09.014
79. Hernando MD, Fernández-Alba AR, Tauler R, Barceló D (2005) Toxicity assays applied to wastewater treatment. Talanta 65:358–366. https://doi.org/10.1016/j.talanta.2004.07.012
80. Zhang J, Zhang Y, Liu W, Quan X, Chen S, Zhao H, Jin Y, Zhang W (2013) Evaluation of removal efficiency for acute toxicity and genotoxicity on zebrafish in anoxic–oxic process from selected municipal wastewater treatment plants. Chemosphere 90:2662–2666. https://doi.org/10.1016/j.chemosphere.2012.11.043
81. Dehghani M, Mahdavi P, Tyagi I, Agarwal S, Kumar Gupta V (2016) Investigating the toxicity of acid dyes from textile effluent under UV/ZnO process using *Daphnia magna*. Desalin Water Treat 57:24359–24367. https://doi.org/10.1080/19443994.2016.1141327
82. Gonçalves AA, Gagnon GA (2011) Ozone application in recirculating aquaculture system: an overview. Ozone Sci Eng 33:345–367. https://doi.org/10.1080/01919512.2011.604595